Ultimate moment capacity of 50 m ultra-high performance fiber reinforced concrete composite box girder

Tsas-Orgilmaa Makhbal[1],* (iD), Sang Mook Han[2]

[1] *School of Civil Engineering and Architecture of Mongolian University of Science and Technology, Ulaanbaatar, Mongolia*
[2] *Civil Engineering Department of Kumoh National Institute of Technology, Gumi, South Korea*
Correspondence author. Email: tsasorgilmaa@must.edu.mn, ORCID: 0000-0002-1825-0097

ABSTRACT

The objective of this study described in this paper is to grasp the ultimate moment capacity of 50 m prestressed ultra-high-performance fiber-reinforced concrete (UHPFRC) composite box girder. The uniqueness of the prestressed UHPFRC composite box girder is no longitudinal reinforcement and no stirrups in two webs and lower flanges. In order to predict the flexural behavior of large-scale UHPFRC composite box girders, the current knowledge of UHPFRC properties and modelling tools is to be developed. The UHPFRC composite box girder consists of three segments UHPFRC U-shaped girder, UHPFRC deck plate, reinforced high-strength concrete (HSC) slab. The steel fiber 1.5% of volume fraction was added to ultra-high-performance concrete (UHPC) to induce ductile behavior in the girder. In total, 146 tendons are installed in the upper and lower flanges of U-shaped girder to cause flexural strength. A simple assumption of composite box girder was considered for a U-shaped girder, UHPFRC deck plate, HSC slab. Equivalent rectangular stress blocks are derived based on compressive and tensile constitutive laws of UHPFRC and HSC. The instantaneous prestress loss was calculated by the analytical method. The ultimate moment capacity of the composite box girder is evaluated with a modified analytical model, which has strain-softening behavior in tension. The result of ultimate moment capacity shows high flexural stiffness.

Keywords: *flexural behavior, bridge, girder, stress block, prestress loss*

1. INTRODUCTION

Ultra-High-Performance Concrete (UHPC) consists of a significantly compact cementitious matrix and high amount of slender steel fibers. UHPC shows good durability, high resistance in chemical reactions [1], high compressive strength ≥120 MPa, high tensile strength ≥4 MPa [2]. Due to its significant features the UHPFRC is applicable under heavy load traffic even in extreme environmental conditions. From the first UHPC road bridge application the Bourg-les-Valence bridge [1] to present, numerous projects have been carried out worldwide.

Although numerous UHPFRC applications have been implemented during over two decades the studies of large-scale structures behavior of UHPC are still not exhausted. The experimental studies of flexural behavior of prestressed UHPFRC girders were investigated by B.Graybeal [2] for I and Pi-shaped girders, by Norio [4] for I and U-shaped girders, by In-Hwan Yang [5] for T-girders, by Jeong Min Seong [6] for segmental box girders, by Lee Seung-Jae [7] for U-shaped segmental girders, by Xiang-Guo Wu [8] for UHPC-Normal Strength Concrete composite I-girders, by Guo Qing-Young [9] for segmental box shaped girders. However, abovementioned studies contribute to a more realistic understanding about flexural behavior of prestressed, steel fiber reinforced UHPFRC girders, more studies are needed for large-scale structures. The UHPFRC exhibits a compressive stress-strain relationship that is nearly linear to high stress levels and more closely resembles a triangular stress distribution of conventional concrete.

Although this behavior could be assumed for through a modification of the parameters of the rectangular stress

block, these design codes currently do not contain provisions allowing the proper modifications to occur. The UHPFRC exhibits a sustained tensile capacity after cracking to high tensile strain levels [2],[5]. Code-based ultimate flexural capacity calculations assume that the concrete carries no tensile force, thus these calculations may be significantly in error if applied to UHPFRC. Because of the above reasons, rectangular stress block approximation and associated analytical methods to predict the behavior of UHPC girders may not be warranted. Xian Guo Wu considered on a simplified equivalent tensile rectangular stress block in order to calculate a precise evaluation of the ultimate limit state of reinforced UHPFRC I girder and reinforced UHPFRC – normal concrete composite girder [8].

The flexural analytical study of post-tensioned, steel reinforced UHPC structures, which have been considered on tensile behavior was performed by several researchers [5][6][8][11][12]. The flexural strength predicted by the analytical analysis conceived experimental results. These studies contributed to more realistic understandings of the flexural behavior of steel reinforced UHPFRC large-scale structures.

The purpose of this study is to predict the ultimate moment capacity of 50 m UHPFRC composite box girder by using rectangular stress blocks of HSC and UHPFRC. A brief introduction of the composite box girder and stress blocks of constitutive laws of HSC and UHPFRC are introduced in Section.2, Section.3 and Section.4, respectively. The calculation of ultimate moment capacity of UHPFRC composite box girder will be assumed in Section 5.

2. GEOMETRY DESIGN OF 50 M UHPFRC COMPOSITE BOX GIRDER

The 50 m span UHPFRC Composite box girder consists of a UHPFRC U-shaped girder, UHPFRC deck slab 50x2500x50000 (thickness, width and length) mm and HSC reinforced slab 240x2500x50000 (thickness, width and length) mm.

The 50 m span UHPFRC U-shaped girder consists of three segments, which were integrated at two joint sections such as scheme (17+16+17) m. The 50 m span UHPFRC U-shaped girder is designed with prestressing tendons 2x7 and 6x22 tendons in upper and lower flanges respectively. Lower tendons were indicated T1, T2, T3, T4, T5, T6 and upper tendons were indicated left T7 and right T7. The feature of U-girder is not reinforced longitudinal and transverse direction except from 0 m to 4 m reinforcement of anchoring zone. The U-shaped girder was connected to UHPFRC deck plate and high strength concrete (HSC) slab by shear key and bar connectors.

The creation of the 50 m span UHPFRC composite box girder consists of two main stages. The first stage of creation is fabrication and transportation of UHPFRC segments and deck plates at factory. The second is creating a shape of composite box girder with connection by glued joints and post-tensioning in Structural Laboratory of KICT, South Korea. After post-tensioning of tendons grouting was injected into sheaths and cured with heat treatment.

3. COMPRESSIVE AND TENSILE BEHAVIOR AND STRESS BLOCKS OF HSC AND UHPFRC

In this section the compressive behavior of HSC, compressive and tensile behaviors of UHPFRC are considered. The UHPFRC shows post-peak behavior after reaching peak points of compressive and tensile strength due to steel fiber reinforcement. Thus, obtaining post-peak behavior of compressive and tensile behaviors is an important step to create stress blocks. In addition, stress blocks of compressive behavior of HSC and compressive and tensile behavior of UHPFRC based on constitutive laws. Detailed calculation of compressive and tensile behaviors and their stress blocks were studied in previous research [14].

3.1 Equivalent Stress Block of Compressive Behavior of HSC

The compressive uniaxial stress-strain relationship and elasticity modulus of HSC were calculated based on the model **Error! Reference source not found.** and shown in Table.1.

$$f_{cu,hsc} = 44 \text{ MPa} , E_{hsc} = 30008 \text{ Mpa}$$

The coordinate of the resultant neutral center of compressive behavior of HSC can be written as:

$$e_{uce,hsc} = 1.78 \times 10^{-3}$$

$$f_{uce,hsc} = 34.79 \text{ MPa}$$

The compressive behavior and rectangular stress block of HSC are illustrated in Fig. 1. This stress block is valuable for calculating ultimate moment capacity and analysis of finite element model.

Table 1. Stress-strain relationship of compressive behavior of HSC [14]

ε	f, MPa
0.001	26.31
0.0012	29.94
0.0014	32.93
0.0016	35.30
0.0018	37.10
0.002	38.40
0.0022	39.27
0.0024	39.78
0.0026	39.99
0.0028	39.95
0.003	39.72
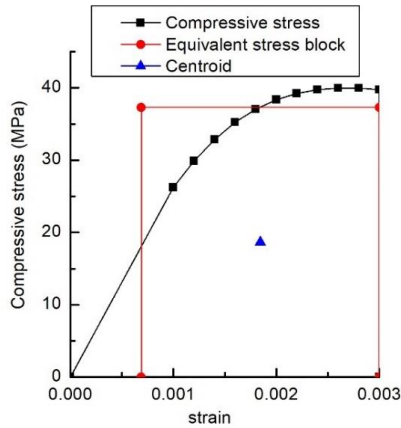
Figure 1. Stress-strain relationship and stress block of compressive stress of HSC [14]

3.2 Equivalent Stress Block of Compressive Behavior of UHPFRC

The compressive behavior of the UHPFRC was modeled by Zhao-Hui Lu et al (2010) [16]. This model can represent the post-peak behavior of UHPC under compression and defined stress-strain relationship based on empirical equations. In order to create stress-strain relationship of compressive behavior, the elasticity modulus of of UHPFRC was calculated based on B. Graybeal's (2007) empirical expression [17]. Fig.2 shows stress-strain relationship of compressive behavior and rectangular stress block of UHPFRC.

$f_{ck} = 135$ Mpa – compressive strength of UHPFRC
$E_0 = 44617$ MPa – elasticity modulus of UHPFRC

Table.1 summarized values of stress-strain relationship of compressive behavior of UHPFRC.
The coordinates of the resultant neutral center can be written as:
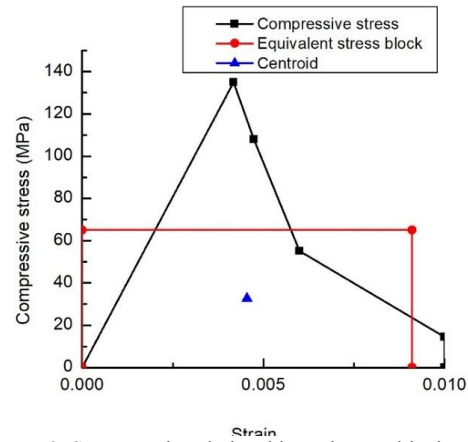
$e_{uc} = 4.55 \times 10^{-3}$
The height of rectangular stress block:
$f_{uce} = 65.1$ MPa

Table 2. Stress-strain relationship of compressive behavior of UHPC [14]

ε_0	f_c^I, MPa
0.00418	135
ε_2	f_2, MPa
0.00474	108
ε_3	f_3, MPa
0.006	55.1
ε_4	f_4, MPa
0.01	14.56

The compressive behavior and rectangular stress block of UHPFRC are shown in Fig. 2.

Figure 2. Stress-strain relationship and stress block of compressive stress of UHPFRC [14]

3.3 Equivalent Stress Block of Tensile Behavior of UHPFRC

The tensile behavior was modeled by tensile law of Ultimate Limit State of AFGC Recommendations on Ultra High Performance Fibre Reinforced Concretes (2013) [15] based on experimental result of flexural tensile strength.

The coordinates of the rectangular stress block of tensile behavior of UHPC:

$e_{ut} = 9.504 \times 10^{-3}$

The height of the rectangular stress block of tensile behavior of UHPC:

$f_{ute} = 13.401$ MPa

Table 3. Stress-strain relationship of tensile behaviour of UHPC. [14]

$\varepsilon_{U,el}$	f_{tfk}, MPa
0.00065	18
$\varepsilon_{U,peak}$	f_{tfk}, MPa
0.0049	18
$\varepsilon_{U,1\%}$	$f_{tf,1\%,k}$, MPa
0.0152	6.35
$\varepsilon_{U,lim}$	$f_{U,lim}$, MPa
0.03	0

This value $f_{ute} = 13.401$ MPa will be used for the ultimate flexural loading capacity and finite element analysis.

Tensile behavior and area of resultant moment about vertical axis of tensile stress block of UHPC are shown in Fig. 3.
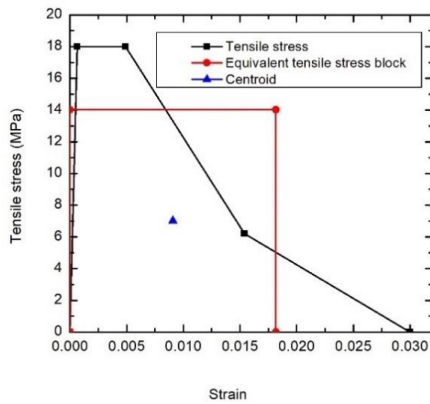
Figure 1. Stress-strain relationship and stress block of tensile stress of UHPFRC [14]
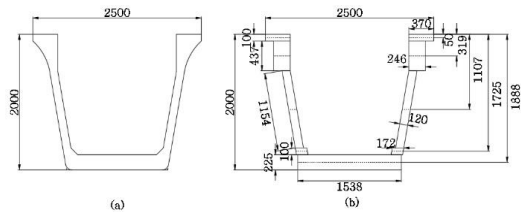
4. PRESTRESS LOSS OF POST-TENSIONED UHPFRC U GIRDER

### 4.1 Cross section properties of U-shaped girder

UHPFRC box girder consists of three segments which were prepared in a factory. The segments were precasted in May 2017 and combined in a U girder in September 2017. Therefore, only instantaneous prestress loss was assumed in this study. Because of the short-term experiment, the time-dependent loss was ignored. The properties of a cross section such as an area, a first moment of area, a moment of inertia, coordinates of centroid and eccentricities of tendons were calculated for determining prestress loss caused in post-tensioned tendons

Fig.4 and Fig.5 show cros-section and simple cross-section and positions of tendons of U-shaped girder.

Area of cross section:

$A_{c,u} = 0.947 \times 10^6$ mm^2

First moment of area: $S_y = 1.092 \times 10^9$ mm^3

Moment of inertia:

$I_{c,u} = 3.575 \times 10^{10}$ mm^4

Squared radius of gyration: $r^2 = 3.275 \times 10^4$ mm^2

Coordinates of centroid: $x_{c,u} = 0$; $y_{c,u} = 1152.96$ mm

Distance from the centroid to extreme top/bottom edge of U-girder:

$y_1 = y_c = 1152.96$ mm

$y_2 = 847.04$ mm

Eccentricity of tendons

At support

$e_{et} = 902.96$ mm – for T7 tendons in top flange

$e_{eb1} = 202.96$ mm – for T1,T2,T3 tendons in bottom flange

$e_{eb2} = 297.04$ mm – for T4,T5,T6 tendons in bottom flange

At midspan

$e_{ct} = 1042.96$ mm – for T7 tendons in top flange

$e_{cb1} = 734.04$ mm – for T1,T2,T3 tendons in bottom flange

$e_{cb2} = 730$ mm – for T4,T5,T6 tendons in bottom flange

Figure 2. U girder cross section: (a) at midspan, (b) transformed cross section at midspan
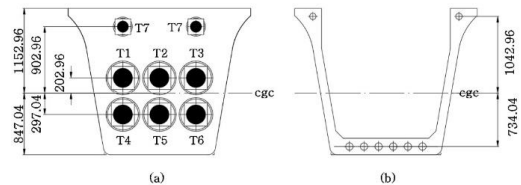
Figure 3. Eccentricity of tendons of U girder (a) at support, (b) at midspan

4.2 Instantaneous Loss

Post-tensioned elements have two groups of prestress loss including instantaneous loss and time dependent loss. Because of laboratory study, the only instantaneous loss will be considered for this composite box girder. The analytical computation of instantaneous loss of prestress

is followed by KCI Structural concrete Design Code [3]. The instantaneous loss of prestress comprises of losses due to elastic shortening loss, anchorage seating loss and loss due to friction.

According to the material property of seven wire strand yield strength of SWPC 7A (15.2mm) tendon is determined as $f_{py} = 1471$ N/mm2 and tensile strength is $f_{pu} = 1730$ N/mm2. Based on ACI maximum permissible stresses prestress transfer must be less than $0.82 \times f_{py} = 1206$ N/mm2 and $0.74 \times f_{pu} = 1280$ N/mm2. Therefore, $0.82 \times f_{py} = 1206$ N/mm2 is assumed for transferring stress in this case. Prestressed bundles are bonded to the sheath.

The summary of instantaneous loss, jacking force for a bundle of strands and jacking force for a single strand are illustrated in Table.4, respectively.

**Table 4.** Summary of prestress loss and jacking force

Position	Unit	T7	T1, T2, T3	T4, T5, T6
Sum of instantaneous loss, Δf_{pim}, N/mm²				
At prestressing	N/mm²	318.72	227.70	219.76
At midspan	N/mm²	270.87	183.59	172.77
At right	N/mm²	324.17	261.42	235.20
Jacking force for a bundle, P_j, KN				
At prestressing	KN	861.46	2985.2	3009.42
At midspan	KN	912.55	3119.78	3152.81
At right	KN	856.17	2882.29	2962.31
Jacking for for a tendon, P_j, KN				
At prestressing	N/mm²	123.07	135.69	136.79
At midspan	N/mm²	130.36	141.81	143.31
At right	N/mm²	122.31	131.01	134.65

5. ULTIMATE MOMENT CAPACITY OF 50 M UHPFRC COMPOSITE BOX GIRDER

Traditionally, designing for bending and normal force in reinforced and prestressed concrete is carried out based on the assumption that plane sections remain plane and that there is a rigid bond between concrete and reinforcement. The tensile strength of the concrete is ignored. The corresponding stress-strain curves are used in the design of the cross-section for concrete in compression and for the reinforcement. Including fibers as additional reinforcement means that these design principles must be extended [10]. Therefore, stress blocks of constitutive laws of compressive and tensile behaviors of HSC and UHPFRC were considered in Section 3.

5.1 Cross section and material properties of composite box girder

To simplify the calculation of ultimate moment capacity, the cross-section at midspan of the box girder was transferred to a simple section. The simple section's assumption of composite box girder is shown in Fig. 6.
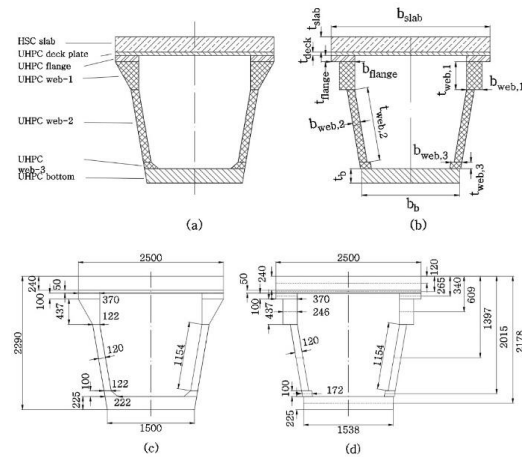
Figure 4. Cross section of composite box girder at midspan

Characteristics of simple section:
First moment of area: $S_{x,b} = 0$ – because of symmetry, $S_{y,b} = 1.471 \times 10^9$ mm³
Coordinates of centroid of box girder:
$x_{c,b} = 0$; $y_{c,b} = 880.06$ mm
$y_{1,b} = y_{c,b} = 880.06$ mm, $y_{2,b} = 1409.936$ mm
$e_{ct} = 480.064$ mm, $e_{cb1} = e_{cb2} = 1296.94$ mm
Moment of inertia of gross section: $I_g = 3.866 \times 10^{10}$ mm⁴,
Squared radius of gyration: $r^2 = 2.312 \times 10^4$
$e_p = 26.27$ mm
Moment of inertia of box girder respect to y axis:
$I_{y,b} = 2.466 \times 10^{12}$ mm⁴
Material characteristics of girder:
$V_f = 1.5\%$, - volume fraction of steel fiber
$L_f = 16$ mm and $L_f = 19$ mm - length of steel fiber
$D_f = 0.16$ mm - diameter of steel fiber
$\alpha = 0.75$ – effect factor of fiber shape
$f_{ck,uhpc} = 135$ MPa – compressive strength of UHPC
$f_{tk,uhpc} = 18$ MPa – flexural tensile strength of UHPC
$E_{uhpc} = 44617$ MPa – elasticity modulus of UHPC
$f_{ckhsc} = 40$ MPa – compressive strength of high strength concrete (HSC)
$E_{hsc} = 30008$ MPa – elasticity modulus of high strength concrete (HSC)

$E_s = 205940$ MPa – elasticity modulus of steel reinforcement

$f_{pu} = 1730$ MPa – breaking strength of tendon SPW7A

$f_{py} = 1471$ MPa – yielding strength of tendon SPW7A

$E_p = 200000$ MPa – elasticity modulus of tendon SPW7A

$A_{p1} = 138.7$ mm^2 – cross sectional area of unit tendon

$n_b = 22$- number of lower tendon in one duct

$N_b = 6$ – number of lower duct

$A_{pb} = 18308.4$ mm^2 – cross sectional area of lower tendons

$n_t = 7$- number of upper tendon in one duct

$N_t = 2$ – number of upper duct

$A_{pt} = 1941.8$ mm^2 – cross sectional area of upper tendons

5.2 Ultimate moment capacity of composite box gider

The girder shows flexural behavior, Hence, the compression flange thickness $h_{slab} + h_{deck}$ is less than neutral axis depth c and equivalent rectangular block depth a, the section can be treated as a flanged section as in Fig. 7.
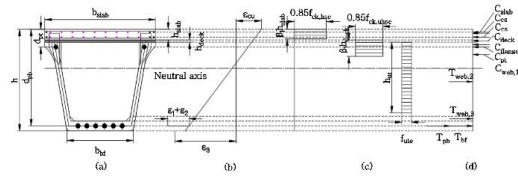
Figure 5. Stress and strain distribution across girder depth. (a) cross section, (b) strains, (c) actual stress block, (d) assumed equivalent stress block.

In this case, ultimate moment capacity must be a moment respected by neutral axis of box girder.

According to the Fig. 7, summing up all forces:

$$T_{web,2} + T_{web,3} + T_{bf} + T_{pb} = C_{slab} + C_{deck} + C_{flange} + C_{web,1} + C_s + C_{pt} \qquad (1)$$

Where,

T_{pb} – total prestressing force in bottom flange

$$T_{pb} = A_{pb}f_{ps} \qquad (2)$$

$T_{web,2}$ – part of force in the web

$$T_{web,2} = A_{web,2}f_{ut,uhpc} \qquad (3)$$

$T_{web,3}$ – part of force in the web

$$T_{web,3} = A_{web,3}f_{ut,uhpc} \qquad (4)$$

T_{bf} – total force in bottom flange

$$T_{bf} = A_{bf}f_{ut,uhpc} \qquad (5)$$

C_{slab} – total force in top slab

$$C_{slab} = 0.85f_{c,hsc}^I b_{slab}h_{slab} \qquad (6)$$

C_{deck} – total force in deck plate

$$C_{deck} = 0.85f_{c,uhpc}^I b_{deck}h_{deck} \qquad (7)$$

C_{flange} – total compressive force in flange

$$C_{flange} = 0.85f_{c,uhpc}^I b_{flange}h_{flange} \qquad (8)$$

C_{cs} – total force of reinforcement steel in slab

$$C_{cs} = C_{cs,t} + C_{cs,b} \qquad (9)$$

$C_{cs,t}$ – total force of upper reinforcement steel in slab

$$C_{cs,t} = A_{st}f_s \qquad (10)$$

$C_{cs,b}$ - total force of lower reinforcement steel in slab

$$C_{cs,b} = A_{sb}f_s \qquad (11)$$

C_{pt} – total prestressing force of top prestressing tendons

$$C_{pt} = A_{pt}f_{ps} \qquad (12)$$

$$a = \beta_1 c = \Big(A_{pb}f_{ps} - \big(A_{pt}f_{ps} + A_s f_y + 0.85f_{c,hsc}^I b_{slab}h_{slab} + 0.85f_{c,uhpc}^I b_{deck}h_{deck} + 0.85f_{c,uhpc}^I b_{flange}h_{flange} \big) \Big) / 0.85f_c^I b_{slab} \qquad (13)$$

Prestress calculation based on strain:

$P_{et} = 1815.8$ KN , $P_{eb1} = 9359.4$ KN , $P_{eb2} = 9458.4$ KN,

$A_{pt} = 970.9$ mm^2 , $A_{pb1} = 3051.4$ mm^2 , $A_{pb1} = 3051.4$ mm^2

The effective prestress strain after transferring jacking force

$$\varepsilon_1 = \frac{P_e}{E_p A_p} \qquad (14)$$

$\varepsilon_1 = 5.095 \times 10^{-3}$

The strain of decompressed condition by external force:

$$\varepsilon_2 = \frac{P_e}{A_c E_c}\Big(1 + \frac{e_p^2}{r_c^2}\Big) \qquad (15)$$

$\varepsilon_2 = 2.849 \times 10^{-4}$

Checking by cross section of flange:

Assume that the stress $f_{ps} = 1206$ MPa

$a = \beta_1 c$, $c = \frac{a}{\beta_1}$, $\beta_1 > 28$ MPa

$$\beta_1 = 0.85 - 0.007(f_{ck} - 28) \qquad (16)$$

The increment of strain due to overload to the ultimate:

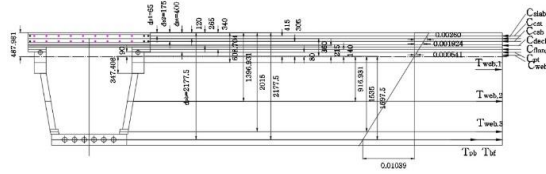$$\varepsilon_3 = \varepsilon_{cu}\Big(\frac{d_p - c}{c}\Big) \qquad (17)$$

The total strain

$$\varepsilon_{ps} = \varepsilon_1 + \varepsilon_2 + \varepsilon_3 \qquad (18)$$

$$\varepsilon_{py} = \frac{f_{pu}}{E_p} \qquad (19)$$

Based on the approximation method of equilibrium position of total compressive and total tensile forces were calculated accurately. This point was determined at the value of c = 487.981 mm from the top of girder. (Fig. 8)

Figure 6. Strain and stress distribution, c=487.981 mm

The strain of decompressed condition by external force when c=487.981 mm:

$\varepsilon_1 = 5.095 \times 10^{-3}$
$\varepsilon_2 = 2.849 \times 10^{-4}$
$\varepsilon_3 = 1.039 \times 10^{-2}$

$\varepsilon_p = 0.0158, \varepsilon_{py} = 0.00865$
$\varepsilon_p = 0.0158 > \varepsilon_{py} = 0.00865$
Total compression force: $\sum C = 44388.07$ KN
Total tensile force: $\sum T = 44388.07$ KN
$\sum C = 44388.07$ KN $= \sum T = 44388.07$ KN

According to the calculation the position of neutral axis is determined when c = 487.981 mm. Hence, the ultimate moment capacity is calculated by Eq (20).

Ultimate moment:

$$M_n = A_{cc} \times \sum f_c y_c + A_{ct} \times \sum f_{ct} y_t + A_p \times f_p \times y_p \quad (20)$$
$$M_n = 83228 \text{ KNm}$$

CONCLUSION

The purpose of this study is to predict the ultimate moment capacity of 50 m UHPFRC composite box girder by the method of ultimate limit state of the prestressed flexural element.

Ultimate moment capacity of the 50 m UHPFRC composite box girder was determined based on compressive and tensile stress blocks of UHPFRC and compressive stress blocks of HSC and instantaneous prestress loss of post-tensioned U-shaped UHPFRC girder.

Because of material properties the equivalence of compressive and tensile forces exists when the c=487.981 mm.

The post-tensioned UHPFRC composite box girder shows high stiffness, although no stirrups and no longitudinal bars in two webs and lower flange.

REFERENCES

[1] Ultra high strength concrete, Heft 561, Berlin, 2008.

[2] B. Graybeal, Characterization of the behavior of ultra-high performance concrete, Maryland, 2005.

[3] Korea Concrete Institute, Design Recommendations for Ultra-High Performance Concrete K-UHPC, KCI-M-12-003, Seoul, Korea, 2012.

[4] H.A.Okuma, K.Nishikawa, I.Iwasaki, and T.Morita, The first highway bridge applying ultra high strength fiber reinforced concrete in Japan, 7th International Conference on short and medium span bridge, Montreal, Canada, (2006), pp. 1857-1865.

[5] In-Hwan Yang, Changbin Joh, and Kim Byung-Suk, Flexural strength of large-scale ultra high performance concrete prestressed T-beams, Canadian Journal of Civil Engineering, 38 (2011), pp. 1185-1195, https://doi.org/10.1139/l11-078

[6] Min-Seon Jeong, Park Sung-Yong, and Han Sang-Mook, Ductile behavior of Ultra High Performance Fiber Reinforced Concrete segmental box girder, Journal of the Korean Recycled Construction Resources Institute, 5 (2017), pp. 290-297.

[7] Lee Seung-Jae, M. Tsas-Orgilmaa, Kim Sung Tae, and Han Sang Mook, Flexural behavior of segmental U-girder and composite U-girder using Ultra High Performance Concrete, Journal of The Korean Recycled Construction resources Institute, 5 (2017), pp. 282-289.

[8] Xiang-Guo Wu, Structural behavior analysis of Ultra-High Performance Prestressed Concrete girder, Department of Civil engineering, Graduate School, Kumoh National Institute of Technology, Gumi, Korea, 2008.

[9] Guo Qing-Yong, Flexural Behavior of Prestressed Ultra High Performance Concrete segmental box girder, Department of Civil Engineering, Kumoh National Institute of Technology, Gumi, Korea, 2011.

[10] James K. Wight, James G. MacGregor, Reinforced Concrete Mechanics and Design, Singapore, Pearson education South Asia, 6E (2012).

[11] B. Graybeal, and M. Asce, Flexural behavior of an Ultra High Performance Concrete I-girder", Journal of Bridge Engineering ® ASCE, 13 (2008), pp. 602-610. https://doi.org/10.1061/(ASCE)1084-0702(2008)13:6(602)

[12] Yoo Doo-Yeol, and Yoon Young-Soo, "Structural performance of ultra-high-performance concrete beams with different steel fibers", Engineering Structures, 102 (2015), pp. 409-423. https://doi.org/10.1016/j.engstruct.2015.08.029

[13] Doo-Yeol Yoo, and Young-Soo Yoon, A review on structural behavior, Design, and Application of Ultra-High-Performance Fiber-Reinforced Concrete, International Journal of Concrete Structures and Materials, 10 (2016), pp. 125-142. https://doi.org/10.1007/s40069-016-0143-x

[14] M. Tsas-Orgilmaa, Constitutive laws of compressive and tensile behavior of UHPFRC, Proceeding of Mongolian University of Science and Technology, 21-9 (2021), pp 159-165.

[15] AFGC Recommendations on Ultra High Performance Fiber-Reinforced Concretes (UHPFRC), France, 2013.

[16] Lu Zhao-Hui, Zhao Yan-Gang, Empirical stress-strain model for unconfined high-strength concrete under uniaxial compression, Journal of Materials in Civil Engineering, 22 (2010), pp. 1181-1186. https://doi.org/10.1061/(ASCE)MT.1943-5533.0000095

[17] B.Graybeal, Compressive Behavior of Ultra-High-Performance Fiber-Reinforced Concrete, ACI Materials Journal, 104 (2007), pp. 146-152. https://doi.org/10.14359/18577